Enhanced nonvolatile resistive switching in dilutely cobalt doped TiO 2

Kashinath A. Bogle, Mukesh N. Bachhav, Meenal S. Deo, Nagarajan Valanoor, and Satishchandra B. Ogale

Enhanced nonvolatile resistive switching in dilutely cobalt doped TiO$_2$

Kashinath A. Bogle,[1] Mukesh N. Bachhav,[1] Meenal S. Deo,[1] Nagarajan Valanoor,[2] and Satishchandra B. Ogale[1,a)]

[1]*Physical and Materials Chemistry Division, National Chemical Laboratory, Pune 411008, India*
[2]*School of Materials Science and Engineering, University of New South Wales, Sydney 2052, Australia*

Incorporation of dilute concentration of dopant having a valence state different than that of the host cation enables controlled incorporation proximity vacancy defects for local charge balance. Since nonvolatile resistive switching is a phenomenon tied to such defects, it can be expected to be influenced by dilute doping. In this work, we demonstrate that enhanced nonvolatile resistive switching is realized in dilutely cobalt doped TiO$_2$ films grown at room temperature. We provide essential characterizations and analyses. We suggest that the oxygen vacancies in the proximity of immobile dopants provide well distributed anchors for the development of systematic filamentary tracks. © 2009 American Institute of Physics. [doi:10.1063/1.3263713]

The phenomenon of resistive switching (RS) has attracted significant attention recently in view of its potential for nonvolatile memory applications (resistive random access memory). It implies a sudden jump between two resistive states, namely a highly resistive (OFF) state and low resistive (ON) state, driven by an applied voltage. This phenomenon has been demonstrated in different types of inorganic, organic, and polymeric materials; including a range of transition metal oxides, such as TiO$_2$, NiO, CoO, PCMO, etc.[1–14] The physical origin of the switching mechanism is still a subject of ongoing debate, though it is suggested to be closely related to the formation and rupture of conducting filamentary paths by an applied voltage.

In this work, we adopt a different approach, namely dilute cobalt doping, to manipulate defect states in TiO$_2$ and influence the corresponding RS performance. We note that cobalt supports lower valence (2+,3+) than Ti (4+) and therefore invites controlled incorporation of oxygen vacancies in an intrinsic way for charge balance.

All the Ti$_{1-x}$Co$_x$O$_{2-\delta}$ based metal/metal oxide/metal devices were fabricated on appropriately and thoroughly cleaned $5 \times 10 \times 1.2$ mm^3 quartz substrates using pulsed laser deposition (PLD) with a KrF ($\lambda = 248$ nm) excimer laser at an energy density of 2 J cm^{-2} at 3×10^{-6} Torr background pressure. First, a 100 nm thick Pt film (bottom electrode) was grown on quartz substrate by PLD using 99.9% pure Pt sheet at an energy density of ~4 J cm^{-2}. The films of Ti$_{1-x}$Co$_x$O$_{2-\delta}$ (x=0, 0.015, 0.04, 0.05, and 0.07) having thickness of ~200 nm were grown at room temperature using sintered TiO$_2$ and Co doped TiO$_2$ targets. Since our probe area was larger than what is normally employed (following litho procedures, etc.), we used higher thickness to avoid variability of results due to pinhole problems. We obtained reproducible data for thicker films as reported here. The x-ray diffraction data revealed broad humps as expected for an amorphous (or nanocrystalline) sample. For RS measurements, Cu tip was used as the top contact (configuration: Cu/Ti$_{1-x}$Co$_x$O$_{2-\delta}$/Pt) and the same was biased while the bottom contact was grounded. The change in the resistance from high resistance state (HRS) to low resistance state (LRS) and

LRS to HRS was measured by applying pulses of ±1.0, 1.5, 2.0, and 2.5 V at a read voltage of +0.1 V. Cobalt incorporation and electronic structure of Co in TiO$_2$ matrix was examined by x-ray photoelectron spectroscopy (XPS) measurements on TiO$_2$ and Co doped TiO$_2$ films.

The XPS spectra for TiO$_{2-\delta}$ and Ti$_{0.95}$Co$_{0.05}$O$_{2-\delta}$ films are shown in Fig. 1. The Ti 2$p_{3/2}$, Ti 2$p_{1/2}$, and O 1s peaks are observed at binding energies 458.5, 464.2, and 530.0 eV, which are very close to those observed in the case of bulk TiO$_2$.[15] In the case of the Ti$_{0.95}$Co$_{0.05}$O$_{2-\delta}$ sample, an overall shift of ~0.2 eV toward higher binding energy side is observed which indicates significant change in the electronic character of the film.[16] Deconvolution of the data (Fig. 1) indicates three symmetric peaks represented as P-1 (green color), P-2 (magenta color), and P-3 (blue color). P-1 is known as low binding energy component (LBEC) at 530 eV, which is assigned to O^{2-} bound to Ti^{4+}. P-2 is a high binding energy component (HBEC), which is due to the formation of oxygen vacancies.[17,18] The P-3 is assigned to the adsorbed
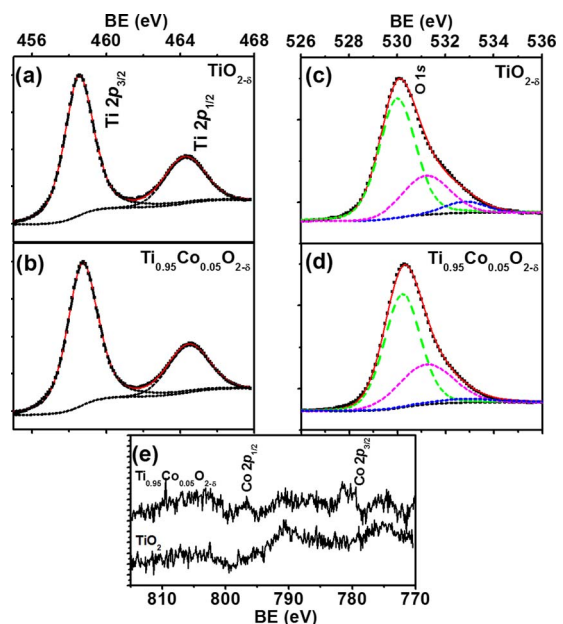
FIG. 1. (Color online) XPS spectra of (a), (b) Ti 2p, (c), (d) O 1s, and (e) Co 2p in TiO$_{2-\delta}$ and Ti$_{0.95}$Co$_{0.05}$O$_{2-\delta}$ films deposited on Pt coated quartz substrate.

a)Author to whom correspondence should be addressed. Tel.: +91-20-25902260. FAX: +91-20-25902636. Electronic mail: sb.ogale@ncl.res.in.

TABLE I. Parameters of the Ti $2p_{3/2}$, Ti $2p_{1/2}$, and O $1s$ XPS peaks of $TiO_{2-\delta}$ and $Ti_{0.95}Co_{0.05}O_{2-\delta}$ films.

Sr. No.	Sample	Element	Line	Fitted Peaks	Peak position (eV)	FWHM	Area
1	TiO_2	O	$1s$	P-1	530.0	1.79	1.22
				P-2	531.2	2.31	0.47
				P-3	532.8	2.00	0.116
		Ti	$2p_{3/2}$	⋯	458.5	1.85	1.78
			$2p_{1/2}$	⋯	464.2	2.55	0.67
2	5%Co:TiO_2	O	$1s$	P-1	530.2	1.73	1.08
				P-2	531.2	2.67	0.55
				P-3	532.8	3.00	0.09
		Ti	$2p_{3/2}$	⋯	458.7	1.93	1.88
			$2p_{1/2}$	⋯	464.4	2.60	0.70

oxygen.[17,18] It is previously reported that the P-2 contribution develops with loss of oxygen.[17,18] Table I summarizes the fitted parameters for both the samples. It reveals that, in the 5% Co doped $TiO_{2-\delta}$ film, the O/Ti ratio is lower by ~10% when compared with the undoped $TiO_{2-\delta}$ film. Furthermore, the relative area under the curve (HBEC/LBEC) is ~0.38 for undoped $TiO_{2-\delta}$, and ~0.51 for 5 at. % Co doped case. The relatively large contribution of the HBEC peak in 5% Co doped $TiO_{2-\delta}$ strongly implies the presence of more oxygen vacancies, which is consistent with the charge balance argument. The Co contribution for $Ti_{0.95}Co_{0.05}O_{2-\delta}$ case is presented in Fig. 1(e) along with the spectrum for undoped TiO_2. Due to low dopant concentration, the signal to noise ratio is rather low. The binding energies for Co $2p_{3/2}$ and $2p_{1/2}$ are observed at 781.4 and 796.8 eV, respectively. This indicates that the cobalt in $Ti_{1-x}Co_xO_{2-\delta}$ films is present in the Co^{2+} or Co^{3+} oxidation state. The XPS analysis thus implies that cobalt in the film is in oxidized state and not in the form of cobalt metal.[15] This was further confirmed by the absence of any detectable ferromagnetic signal in the sample.

Figure 2 represents results of the *I-V* measurement under 100 ms pulse induced write-read-erase mode conducted on the devices for several hours. In this, the "write" (i.e., ON state) is made by applying a positive voltage pulse and the "erase" (OFF state) is achieved through erasing the ON state by reversing the polarity. During these measurements, a small read voltage (+0.1 V) was applied to read the states [ON state (write) and OFF state (erase)] of the device.
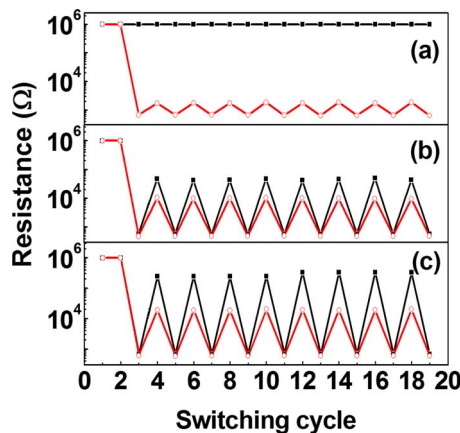

FIG. 2. (Color online) Bipolar RS observed at an applied voltage pulse of ±1 and ±1.5 V at a read out voltage of +0.1 V for (a) $Cu/TiO_{2-\delta}/Pt$, (b) $Cu/Ti_{0.96}Co_{0.04}O_{2-\delta}/Pt$, and (c) $Cu/Ti_{0.95}Co_{0.05}O_{2-\delta}/Pt$ device.

As can be seen in Fig. 2(a) (black line curve, -■-), the $Cu/TiO_{2-\delta}/Pt$ device is in HRS (OFF state) before applying the voltage pulse. When a pulse of +1.0 V is applied, it does not change to the LRS state making the switching action basically inoperative for this voltage, with the device remaining in HRS under repeated application of ±1.0 V pulses. When the measurements are carried out on this device under the same condition but with pulses of ±1.5 V [red line curve in Fig. 2(a), -○-], interesting results are obtained. A pulse of +1.5 V switched the initial HRS to LRS and application of a pulse of −1.5 V restored the resistance value to almost the same initial HRS. The difference between the resistance in the HRS and LRS is of one order of magnitude. Measurements carried out at pulses of ±2 V showed that an applied −2 V pulse switches the initial HRS of the device to LRS, whereas the device remains in the LRS under application of next +2 V pulse. The device was found to be in the LRS under application of further ±2 V pulses, thus being nonswitchable. For the voltage pulses of ±2.5 V, similar behavior was observed with a minor change in resistance.

Similar measurements were done on $Cu/Ti_{1-x}Co_xO_{2-\delta}/Pt$ devices for $x=0.015$, 0.04, 0.05, and 0.07 cases. The characteristics for the case of $x=0.015$ were very similar to the $x=0.0$ case and are not shown here. Similarly, for $x=0.07$, the effect was found to be negligible. Figures 2(b) and 2(c), however, shows the dramatic changes seen in the switching properties for intermediate doping levels of x $=0.04$ and $x=0.05$. The effect was found to be strongest for $x=0.05$ among the cases examined. For this case, a major improvement of more than four orders of magnitude was observed in the difference between the resistance at HRS and LRS under testing at the low voltage of ±1 V [compare black curve in Figs. 2(a) and 2(b), -■-]. Measurements carried out at ±1.5 V also showed excellent switching trend with a difference of three orders of magnitude [red line curve in Fig. 2(b), -○-]. At higher voltage pulsing (±2, ±2.5 V), a poor switching character was noted as expected based on the nature of the phenomenon.

The observed difference in the OFF and ON state resistance value for the $Cu/TiO_{2-\delta}/Pt$ device in our case is lower than that reported by others for the (~20–40 nm thick) TiO_2 films.[7,12,14] A major difference between other data for films grown at higher temperatures and ours is in the OFF state resistance value, whereas, the ON state resistance value is of the same magnitude. Interestingly, the difference found in our $Cu/TiO_{2-\delta}/Pt$ device (at read voltage of +0.1 V and voltage pulses of ±1.5 V) is much closer to that reported by Schroeder *et al.*[13] at a read voltage of +0.3 V and voltage pulses of ±3 V for their 27 nm TiO_2 film deposited also at room temperature using reactive sputtering technique. It has been reported that RS is an intrinsic property of the film and also depends on the interface between the resistive film and the electrode layer.[1] There is always an ultrathin layer of intrinsic oxide on copper, although we give an acid etch before making contact for the measurement. Also, there is a formation of Cu oxide at the interface in the measurement process itself. At low voltage pulses (±1.0 and 1.5 V) during switching OFF to ON, the formation of the conducting filament occurs via propagation of vacancies toward Pt negative electrode and O^{2-} ions toward Cu positive electrode. This leads to an accumulation of O^{2-} ions near top Cu electrode, which results in partial oxidation of the top Cu electrode by absorbing oxygen ions from the film. The oxygen ions can be
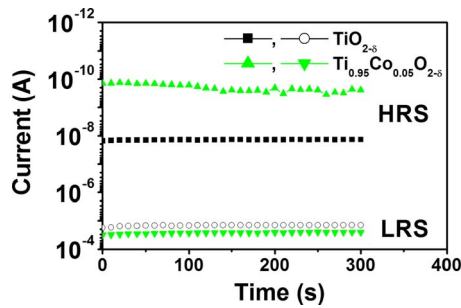
FIG. 3. (Color online) The retention properties of high resistance state and low resistance state of $Cu/TiO_{2-\delta}/Pt$ and $Cu/Ti_{0.95}Co_{0.05}O_{2-\delta}/Pt$ devices at a read voltage of +0.1 V.

withdrawn into the film depending on the electrical force influencing the filament evolution and the precise structural constitution of the material. In the case of TiO_2 films fabricated using conventional sputtering techniques at room or high temperature, the nature (epitaxial or polycrystalline or amorphous) of the film and the defects (oxygen traps) therein play a major role in the formation of conducting filamentary paths. Defects are always present in amorphous or nanocrystalline $TiO_{2-\delta}$ film, which accounts for its relatively good conductivity.[9] Film growth at high temperature (300–400 °C) or postannealing after preparation changes the RS behavior considerably as expected. We avoided high temperature processing (deposition or annealing) to avoid possible effects of cobalt clustering and reduction in the oxygen vacancy defect concentration. In fact, in the devices grown at 300 °C, the resistance ratios between ON and OFF states were found to be 10^1 and 10^2 for TiO_2 and $x=0.05$ $Ti_{1-x}Co_xO_2$ cases, respectively. These data will be discussed separately.

The absence of switching effect in $Cu/TiO_{2-\delta}/Pt$ device at ± 1 V clearly indicates that the process of filament formation is not induced at this voltage. Whereas, at higher voltage (~ 1.5 V in this case) above a certain threshold, repeated switching of the resistance between HRS to LRS to HRS signifies the formation and rupturing of filament. For much higher voltage pulses (± 2 and ± 2.5 V), the applied high voltage stress makes the filamentary paths permanent, hence once the device switches to LRS it remains in that state. Doping of Co in $TiO_{2-\delta}$ at dilute level ($\sim 4-5$ at. %) dramatically improves the switching properties even at the low voltage ± 1 V, which is desirable for applications. This confirms that dilute doping of Co modulates the oxygen vacancy concentration, which results in unusual switching via formation and rupturing of filament at voltage below the threshold voltage. We believe that it is not only important to have more oxygen vacancies but to have them well distributed within the film mimicking the distribution of dopants. The dopants thus serve as chemical anchors for vacancies across which the O^{2-} ions can transport under field stress. Note that cobalt ions would not move under electric field bias at the values used. Hence, the oxygen vacancies induced in their proximity will continue to hold an arrangement across the film thickness that can guide the filament formation process.

Figure 3 compares the results of retention properties of high resistance state and low resistance state of $Cu/TiO_{2-\delta}/Pt$ and $Cu/Ti_{0.95}Co_{0.05}O_{2-\delta}/Pt$ devices at a read voltage of +0.1 V shown for 300 s. We note that our observations showed that similar stability of states persists even

up to 5000 s, the maximum time for which the devices were examined. As can be seen, once the $Cu/TiO_{2-\delta}/Pt$ device is switched to LRS (ON state), the state is retained without any degradation for a long time; moreover, the HRS (OFF state) also shows good retention properties. Similar long term reliable retention properties are also observed for $Cu/Ti_{0.95}Co_{0.05}O_{2-\delta}/Pt$ device (green lines curve in Fig. 3) with small fatigue at HRS (OFF state) that could originate from the detrapped carriers at the interfacial states. These results confirm that the $Cu/Ti_{0.95}Co_{0.05}O_{2-\delta}/Pt$ device has excellent programmability (write-read-erase) for nonvolatile memory device application.

RS has been reported to be closely related to the formation and rupture of conducting track (a fractal shape known as filament).[2,7–11] Although the exact nature of the filament in TiO_2 is not yet clear, the migration of oxygen vacancies (V_o^{2+}) in the vicinity of the interface under applied voltage is suggested to drive RS. Thus, introduction of Co in $TiO_{2-\delta}$ film at diluted concentration provides a controllable way of manipulating the oxygen vacancies via its need to satisfy its valance (Co^{2+}), as well as its contribution to scattering which can enhance the HRS value.[19,20]

Future work will involve explorations involving different metal oxides (switching elements), metallic electrodes, and dopants.

[1] J. J. Yang, M. D. Pickett, X. Li, D. A. A. Ohlberg, D. R. Stewart, and R. S. Williams, Nat. Nanotechnol. **3**, 429 (2008).

[2] S. Baek, D. Lee, J. Kim, S. H. Hong, O. Kim, and M. Ree, Adv. Funct. Mater. **17**, 2637 (2007).

[3] Y. Yang, J. Ouyang, L. Ma, R. J. H. Tseng, and C. W. Chu, Adv. Funct. Mater. **16**, 1001 (2006).

[4] M. Fujimoto, H. Koyama, Y. Nishi, and T. Suzuki, Appl. Phys. Lett. **91**, 223504 (2007).

[5] I. H. Inoue, S. Yasuda, H. Akinaga, and H. Takagi, Phys. Rev. B **77**, 035105 (2008).

[6] A. Sawa, Mater. Today **11**, 28 (2008).

[7] K. Tsunoda, Y. Fukuzumi, J. R. Jameson, Z. Wang, P. B. Griffin, and Y. Nishi, Appl. Phys. Lett. **90**, 113501 (2007).

[8] C. Rohde, B. J. Choi, D. S. Jeong, S. Choi, J. S. Zhao, and C. S. Hwang, Appl. Phys. Lett. **86**, 262907 (2005).

[9] K. M. Kim, B. J. Choi, and C. S. Hwang, Appl. Phys. Lett. **90**, 242906 (2007).

[10] K. M. Kim and C. S. Hwang, Appl. Phys. Lett. **94**, 122109 (2009).

[11] K. M. Kim, B. J. Choi, D. S. Jeong, C. S. Hwang, and S. Han, Appl. Phys. Lett. **89**, 162912 (2006).

[12] C. Yoshida, K. Tsunoda, H. Noshiro, and Y. Sugiyama, Appl. Phys. Lett. **91**, 223510 (2007).

[13] D. S. Jeong, H. Schroder, and R. Waser, Electrochem. Solid-State Lett. **10**, G51 (2007).

[14] M. Fujimoto, H. Koyama, M. Konagai, Y. Hosoi, K. Ishihara, S. Ohnishi, and N. Awaya, Appl. Phys. Lett. **89**, 223509 (2006).

[15] J. W. Quilty, A. J. Shibata, Y. Son, K. Takubo, T. Mizokawa, H. Toyosaki, T. Fukumura, and M. Kawasaki, Phys. Rev. Lett. **96**, 027202 (2006).

[16] S. H. Cheung, P. Nachimuthu, M. H. Engelhard, C. M. Wang, and S. A. Chambers, Surf. Sci. **602**, 133 (2008).

[17] Y. B. Lin, Y. M. Yang, B. Zhuang, S. L. Huang, L. P. Wu, Z. G. Hunag, F. M. Zhang, and Y. W. Du, J. Phys. D: Appl. Phys. **41**, 195007 (2008).

[18] M. Naeem, S. K. Hasanain, M. Kobayashi, Y. Ishida, A. Fujimori, S. Buzby, and S. I. Saha, Nanotechnology **17**, 2675 (2006).

[19] K. A. Griffin, A. B. Pakhomov, C. M. Wang, S. M. Heald, and K. M. Krishnan, Phys. Rev. Lett. **94**, 157204 (2005).

[20] S. R. Shinde, S. D. Sarma, J. R. Simpson, H. D. Drew, S. E. Lofland, C. Lanci, J. P. Buban, N. D. Browning, and S. B. Ogale, Phys. Rev. B **67**, 115211 (2003).